Available online at www.sciencedirect.com
ScienceDirect
Journal of Pharmaceutical and Biomedical Analysis 47 (2008) 95–102
JOURNAL OF PHARMACEUTICAL AND BIOMEDICAL ANALYSIS
www.elsevier.com/locate/jpba

A detailed analysis of biodegradable nanospheres by different techniques—A combined approach to detect particle sizes and size distributions

Christian Augsten [a], Mikhail A. Kiselev [b], Rainer Gehrke [c], Gerd Hause [d], Karsten Mäder [a,*]

[a] *Martin-Luther-University of Halle-Wittenberg, Institute of Pharmacy, 06120 Halle, Germany*
[b] *Frank Laboratory of Neutron Physics, Joint Institute for Nuclear Research, 141980 Dubna, Russia*
[c] *HASYLAB at DESY, 22603 Hamburg, Germany*
[d] *Martin-Luther-University of Halle-Wittenberg, Microscopy Unit of the Biocenter, 06120 Halle, Germany*

Received 12 September 2007; received in revised form 16 December 2007; accepted 17 December 2007
Available online 26 December 2007

Abstract

Poly(D,L-lactide-co-glycolide) nanosupensions as intravenous nanosphere systems were produced by solvent deposition in aqueous Poloxamer 188 solutions. Light scattering techniques were applied to these colloidal systems to characterize particle sizes. Regularly shaped spherical particles were received as proved by freeze fracture replica and small-angle X-ray scattering (SAXS). SAXS was performed using intensive synchrotron radiation. Particle sizes were calculated from the small-angle part of scattering curve that were in good agreement with *z*-average values received from photon correlation spectroscopy (PCS). The flow field-flow fractionation (FlFFF) fractograms in combination with multi-angle light scattering (MALS) allowed an easy detection of maximum particle sizes what is most important for parenteral systems. Furthermore, high quality size distributions were received due to the separation step prior to size characterization. The calculated average size values exhibited a good correlation with *z*-averages determined by PCS. Only for suspensions of broader size distributions, higher deviations were observed. Comparing particle sizes with and without Poloxamer, differences in diameters resulted that were quantified. The additional Poloxamer shell was not able to be removed by an intensive washing during FlFFF focusing and separation. Especially FlFFF/MALS proved to be a valuable tool to characterize the pharmaceutical nanosuspensions in detail what is of great importance especially for controlled drug delivery systems.

Keywords: Nanoparticles; Poly(D,L-lactide-co-glycolide); Particle size distribution; Flow field-flow fractionation; Small-angle X-ray scattering; Photon correlation spectroscopy; Poloxamer

1. Introduction

Biodegradable nanoparticles are able to improve the efficacy and to reduce the toxicity of drugs. They are small enough to be injected intramuscularly and even intravenously. Polyesters like lactic and glycolic acid copolymers have been widely studied for that kind of application, since their degradation products are known to be harmless and they have already received regulatory approval [1]. A quite simple method for producing such nanoparticles is the solvent deposition method [2]. It is possible to receive particles of predictable sizes using that method under selected conditions [3,4].

Stabilizers as poly(vinyl alcohol) or block copolymers of poly(ethylene oxide) and poly(propylene oxide) (Poloxamers) are necessary to allow nanosized particle preparations and to prevent aggregation during storage [5,6]. In the case of intravenous systems, hydrophilic layers of poly(ethylene oxide) (PEG) have been reported to influence the particle surface and to protect them against uptake in liver and spleen [7,8]. This undesired uptake is supported by opsonization resulting in phagocytosis by macrophages of the reticuloendothelial system [7]. Two possibilities for delaying this process by PEG exist: (i) incorporation of PEG-containing amphiphiles in the formulation or

* Corresponding author at: Martin-Luther-University Halle-Wittenberg, Institute of Pharmacy, Wolfgang-Langenbeck-Straße 4, 06120 Halle, Germany. Tel.: +49 345 5525167; fax: +49 345 5527029.
E-mail address: karsten.maeder@pharmazie.uni-halle.de (K. Mäder).

0731-7085/$ – see front matter © 2007 Elsevier B.V. All rights reserved.
doi:10.1016/j.jpba.2007.12.031

(ii) covalent linkage to the particle surface [9]. Covalent attachment creates new substances that have to be approved after a broad toxicology program. In contrast, Poloxamer 188 is a stabilizer that can be simply added to parenteral formulations and already reached regulatory approval state. Therefore, we focused our studies on Poloxamer 188 stabilized poly(D,L-lactide-co-glycolide) (PLGA) nanosupensions.

The particle size and size distribution are key parameters for the performance and safety of nanosuspensions, especially for intravenous systems. Furthermore, they are key parameters for the blood circulation time [10]. Particle size measurements of nanosized materials are not trivial as they appear on the first view. The existence of several species, size distributions, anisotropic shapes, different calculation methodologies and uncertainties of the optical properties make the assessment difficult. It is important to understand, that in most cases physical properties – and not the particle size – are measured. Several methods (e.g. electron microscopy, light scattering, small-angle X-ray scattering (SAXS), field-flow fractionation (FFF)) do exist. They access different properties of the particles. It was therefore the aim of the current study to compare them with respect to the measured size and size distribution, efforts and requirements.

TEM pictures were made to determine the particle shape. In addition, we applied several light scattering techniques to these colloidal systems that allowed a particle size characterization. Photon correlation spectroscopy (PCS) data were used as reference. Furthermore, small-angle X-ray scattering (SAXS) and flow field-flow fractionation (FlFFF) combined with multi-angle light scattering (MALS) were applied to selected nanosuspensions.

FlFFF is a powerful tool to separate molecules, nanoparticles and small microparticles [11]. By the use of this technique one is able to separate a wide field of pharmaceutical substances as polysaccharides, proteins, viruses, bacteria and other nanoparticles [12,13]. Despite the great potential of FlFFF in pharmaceutics, only few papers have been published on pharmaceutical nanosphere systems, e.g. [14]. The FlFFF separation behaviour depends on the diffusion properties of the particles. The respective hydrodynamic size can be calculated from elution time using FlFFF theory [15]. However, the retention of the sample can also be influenced by adhesion and charge phenomena, leading to falsified values from FFF theory [16]. Thus, it is more advantageously to couple FlFFF to MALS. Herewith it is possible to determine absolute molar masses of molecules and to achieve the radius of gyration (R_g) for particles of appropriate size [17].

To determine the size of nanoparticles, photon correlation spectroscopy (PCS) is widely used [18]. Assuming spherical particles, hydrodynamic size values can be calculated. It is a relatively fast technique with moderate equipment demand.

Small-angle X-ray scattering is a good choice for a more detailed structure characterization. Compared to visible light based methods, much smaller structures can be resolved due to the short wavelengths of the X-rays. The principles of SAXS are well described [19]. By evaluating the intensity of diffuse scattering at small angles, that method gives information about particle sizes, shapes and surface structures from one to a few thousand nanometres and can be applied on various nanoparticle systems [20]. But just a few articles can be found in the field of characterization of nanoparticles consisting of biodegradable polymers, e.g. [21]. Nanoparticles in medicine are in most cases poor scatterers, as already reported [22]. Therefore, in order to obtain useful data with good statistics an X-ray beam of high intensity with good collimation and a small detectable angle is required (e.g. the small-angle beamline BW4 at Deutsches Elektronen-Synchrotron, DESY).

TEM of freeze fracture replica is a microscopic technique that achieves sufficient resolution within the desired size range to determine the particle shape. This is necessary to allow calculation of geometric sizes from gyration radii.

2. Materials and methods

2.1. Nanoparticle production

The aqueous suspensions of PLGA nanospheres consisted of 0.25%, 0.5% or 1% (w/v) of Purasorb PDLG (briefly Pura PDLG) or Resomer RG 502, 503, 502H, 503H or 504H (briefly Res 50X). The Resomer Polyesters were kindly donated from Boehringer-Ingelheim Pharma GmbH (Ingelheim, Germany) and Purasorb polymers were a kind gift from PURAC Germany (Bingen, Germany). Their respective molar masses are given in Table 1. The particles were produced using the solvent deposition method [2] with a few variations. According to Chacon et al. [4], the polymer was dissolved in acetone and injected automatically in the double amount of water containing 0–4% (w/v) Poloxamer 188 (BASF Ludwigshafen, Germany). This procedure was continued by the evaporation of acetone and a part of water under reduced pressure to the desired volume (40 °C, 200 mbar decreasing slowly to 30 mbar). All suspensions were produced three times at least and measured twice or three times at least (details are given for each measurement technique). Poloxamer 188 was added to some nanosuspensions post-production, as described in the following text.

2.2. Transmission electron microscopy of freeze fracture replica

The TEM samples were cryofixed with a propane jet freezer (JFD 60, BAL-TEC, Liechtenstein) and freeze fractured at −110 °C using a BAF 060 freeze fracture apparatus (BAL-TEC, Liechtenstein). After freeze etching for 1 min, the surfaces were shadowed with platinum (2 nm, shadowing angle 45°) and subsequently with carbon (22 nm, shadowing angle 90°). The replica were floated in sodium chloride (4% Cl) for 30 min, rinsed in distilled water for 5 min and washed in 30% acetone for 30 min. After final washing in distilled water, the replica were mounted on formvar coated copper grids and observed with a transmission electron microscope (EM 900, Carl Zeiss SMT, Oberkochen) operating at 80 kV. Pictures were taken with a Variospeed SSCCD camera SM-1k-120 (TRS, Moorenweis, Germany).

Table 1
Weight (Mw) and number (Mn) average molar masses of poly(D,L-lactide-co-glycolides)

PLGA type	Res 502	Res 502H	Res 503	Res 503H	Res 504H	Pura PDLG
Mw (kDa)	18.6	14.6	40.6	37.0	52.5	43.5
Mn (kDa)	11.4	7.9	25.3	22.5	32.4	20.5

The values were determined by GPC using polystyrene standards. The values for the Resomer polymers were provided by the supplier, the values for Pura PDLG were measured by the authors.

2.3. PCS measurements

The R_H were measured at 25 °C by PCS. They are only described as hydrodynamic radii or diameters (z-averages) within the following text. A HPPS 5002 from Malvern Instruments Limited (Worcestershire, UK) was used. Assuming a spherical system, the Stokes–Einstein relationship was applied, where k_B represents the Boltzmann constant and T the temperature [23]:

$$D = \frac{k_B \cdot T}{6\pi \cdot \eta \cdot R_H}$$

The measurements were performed three times at least, each time with at least 14 single correlation curves. The given error bars display the corresponding standard deviations. The dynamic viscosity η of Poloxamer 188 solutions was determined using Ubbelohde-viscosimeters (Schott, type K1c and 0a) with their respective instrument constants k:

$$\eta = k \cdot (t_{outlet} - F) \cdot \rho$$

Therefore, concentrations of 0.12, 0.30, 0.50, 0.60, 0.75, 1.00, 2.00, 3.00, 4.00 and 10.00 g/100 ml were used. The measurements were performed three times. The outlet time results t_{outlet} were corrected by a few seconds F via Hagenbach to consider the amount of potential energy that is needed to accelerate the liquid. The required density ρ was determined using a Mohr-Westphal weighing machine (Johannes Hammer, Germany).

2.4. SAXS measurements

Scattering curves from BW4 beam line at DORIS (HASYLAB at DESY, Hamburg, Germany) were collected with a wavelength of 0.15 nm at sample-detector distances of 13 and 3 m at a temperature of 27 °C. Example suspensions were selected for measurement. The intensities of corresponding single measurements were accumulated before performing further calculations. The relationship between the scattering angle 2θ and the scattering vector q is given by the relationship for elastic scattering [24] where λ is the wave length:

$$q = \frac{4\pi}{\lambda} \sin\,\theta$$

The X-ray scattering from isolated particles at sufficiently small q-values is described by the Guinier approximation [25] where I_0 is the intensity of X-ray beam at zero scattering angle:

$$I(q) = I_0 \cdot e^{-1/3R_g^2 \cdot q^2}$$

The gyration radius R_g is related to the particle diameter d_{geom} of a sphere as follows [25]:

$$d_{geom} = 2 \cdot \sqrt{\frac{5}{3}} \cdot R_g$$

Values of R_g were calculated from Kratky-Porod plots of $\ln(I(q))$ against q^2 in the range of scattering vectors q from 0.029 to 0.053 nm^{-1}. This range of q determines the homogeneous region of the scattering curve.

2.5. Asymmetrical FlFFF/MALS measurements

The suspensions were separated by asymmetrical FlFFF (Eclipse F and channel from Wyatt Technology Europe, Germany) with a spacer height of 350 μm and a regenerated cellulose membrane (Microdyn Nadir GmbH, Wiesbaden, Germany) of 10 kDa cut off using bidistilled water with 1 g/l sodium dodecyl sulphate as a background solvent. A 2% Poloxamer solution was used as background for the Poloxamer containing nanosuspensions. After flow equilibration, 100 μl of each sample were injected for 2 min during focusing with 0.2 ml/min injection flow and subsequently focused without injection for 1 min. Then the solutions were separated using a three step cross flow rate gradient. The cross flow started from 1 ml/min, decreased to 0.3 ml/min within 8 min and to 0.1 ml/min within 20 min. Then the cross flow was kept constant for 10 min. The detector flow rate was 1 ml/min during all the separation time. The system was connected to a Dawn EOS MALS detector (Wyatt Technology Europe). The Astra software 4.90 was applied using the sphere model [17]. The geometrical sizes were calculated from weight averaged R_g by the formula given above. All measurements were performed at least twice. The given error bars display the corresponding standard deviations.

3. Results and discussion

3.1. TEM

A first view on the produced nanoparticles was presented by the TEM pictures given in Fig. 1. Independent of Poloxamer addition the particles were sphere-like and regularly shaped. The diameters of both exemplarily shown particles were about 100 nm, but they were not necessarily representative because, e.g. a high number of characterized particles would be necessary and fracture can occur not only in the particle centre. A small shell seemed to be visible around the sphere in Poloxamer containing media. But this could not be proved. However, the recognition of the particle shape allowed the use of formulae assuming a spherical system in all light and X-ray scattering calculations.

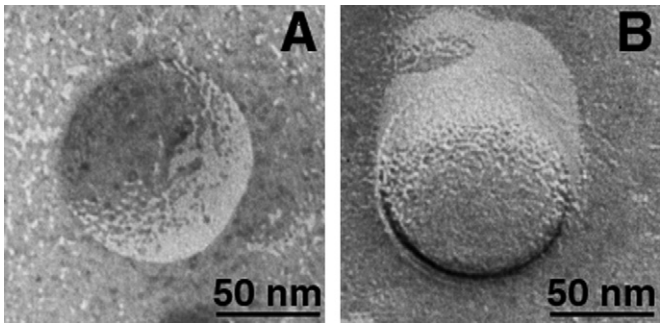

Fig. 1. Freeze fracture replica of 0.5% (w/v) Resomer RG 503 nanoparticles in 0% (w/v) (A) or 2% (w/v) (B) Poloxamer 188 solutions.

3.2. Viscosity and PCS

In contrast to the other used techniques, PCS provided relatively short measuring and evaluation times. Therefore, the following pre-tests concerning the influence of Poloxamer addition were performed using PCS. For this technique the basis of correct hydrodynamic size determination was to reveal dynamic viscosity values of aqueous solutions used for nanoparticle production. The corresponding formula of a polynomial of second degree was calculated to relate Poloxamer 188 concentrations c_{Pol} from 0% up to 10% (w/v) to solution viscosity η_{Pol}:

$$\eta_{Pol} = \eta_{water} + (0.193 \pm 0.004\,\text{mPas}) \cdot c_{Pol} + (0.0128 \pm 0.0004\,\text{mPas}) \cdot c_{Pol}^2 \quad \text{with} \quad R^2 = 0.999$$

The calculated values were used for all further PCS experiments. It can be seen that the effect was strong because without the correction, e.g. for nanoparticles in 2% (w/v) Poloxamer solutions sizes would have been overestimated by a factor of 1.5. Unfortunately, the corresponding viscosity values are rarely given for PCS results in literature, making a comparison to other values difficult. Similar Poloxamer concentrations were used, e.g. by [3,4,26].

First, measurements were performed to test the influence of Poloxamer addition using the correct solution viscosities. The viscosity-corrected PCS results of suspensions of one PLGA type are shown in Fig. 2. Low polydispersity index values (PDI) between approximately 0.05 and 0.1 were found for all systems that indicate a narrow size distribution. In comparison, other parenteral nanosystems as commercial fat emulsions result in PCS PDI values of approximately 0.1 up to 0.25 [18]. Hydrodynamic average diameters between approximately 120 and 140 nm were received which makes an intravenous injection of the particles feasible. If Poloxamer was added to water already before production, the hydrodynamic diameters remained in the same size range between 120 and 140 nm with increasing stabilizer amount. Thus, Poloxamer had no strong influence on the particle formation and the obtained particle size distributions under the examined conditions, regardless whether interfacial turbulence or ouzo effects appeared during production [27,28]. But the literature is not completely uniform in this matter. Stabilizer addition might also be possible post-production [9]. Hence, nanosuspensions were produced by Poloxamer addition after the

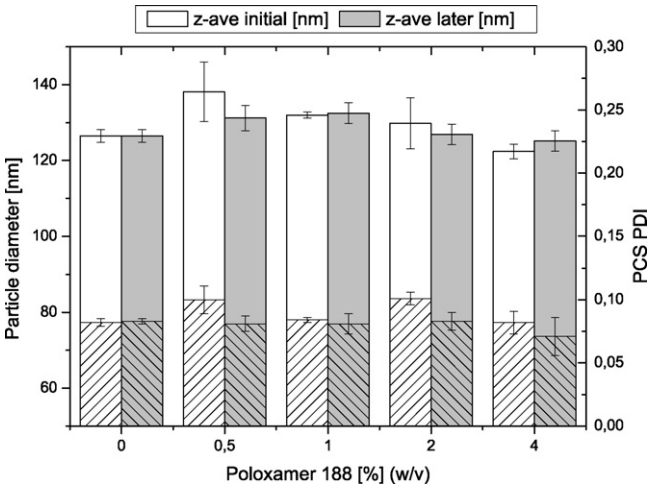

Fig. 2. Hydrodynamic diameters of 0.5% (w/v) Resomer RG 503 nanospheres containing different amounts of Poloxamer 188, added before (initial) or after production (later), corresponding PDI in hatched columns.

nanoparticles had been formed. The PCS results are also given in Fig. 2. Only small deviations in particle size were received between both production processes. For all further experiments the initial use of Poloxamer was applied because Purasorb PLDG required stabilizer addition before production.

3.3. SAXS vs. PCS

A further characterization of selected nanoparticles was performed by SAXS measurements. Two SAXS scattering curves are shown as examples in Fig. 3 where scattering intensity is plotted against the scattering vector. The polydispersity of the nanospheres was relatively low, as can be seen from corresponding PCS data in Figs. 4 and 5. Values were in the range from approximately 0.07 to 0.14, indicating mostly narrow size distributions of the samples. However, the distributions were broad enough to cause a smoothing of the scattering curves. As a result, no minima in the middle q range were detectable in Fig. 3 that allowed an easy size evaluation. This situation is common for many pharmaceutical systems, in contrast to ideal sphere systems described in the literature [24].

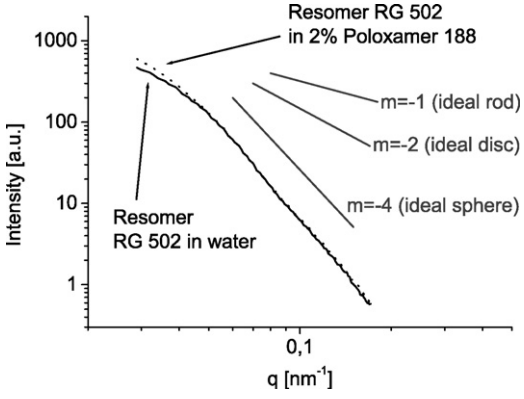

Fig. 3. SAXS scattering curves of 1.0% (w/v) Resomer RG 502 nanoparticles in water without (solid line) or including 2% (w/v) Poloxamer 188 (dotted line), slopes (m) of ideal structure values taken from [32].

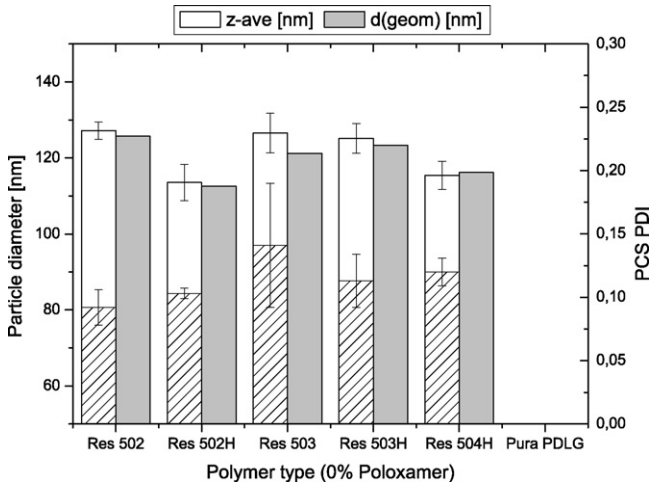

Fig. 4. Hydrodynamic (PCS) and geometric (SAXS) diameters of 1.0% (w/v) nanosuspensions of different PLGA types without Poloxamer 188, corresponding PDI in hatched columns (Pura PDLG demanded Poloxamer addition).

However, structure information could be obtained from the scattering curves by analyzing their behaviour at larger q-values. The curves of all examined systems were parallel at $q > 0.05\,\mathrm{nm}^{-1}$. This vector range was used to achieve information about the particle shape. The curves followed approximately q^{-4} which is predicted for ideal spheres [25].

The scattering curves showed different behaviour at low q values (=very small scattering angles). These smallest scattering angles achieved in the SAXS measurements contained information about the largest detectable structures. In the case of the examined nanoparticles diameters about 120 nm were expected. Thus, the particle diameters were evaluated from these scattering curves at low q values using the Guinier approximation. Fig. 4 shows the particle diameters for nanosphere suspensions without Poloxamer, comparing PCS and SAXS results. The same size relationship was achieved by both methods. That means the received values were in good agreement although the measuring principles were completely different, showing the capability of

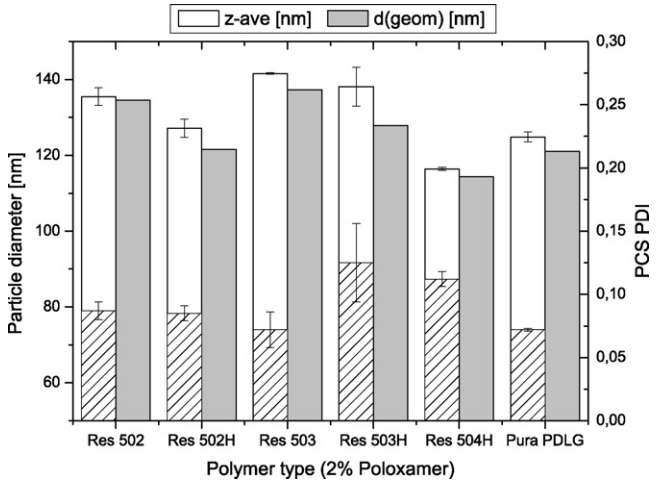

Fig. 5. Hydrodynamic (PCS) and geometric (SAXS) diameters of 1.0% (w/v) nanosuspensions of different PLGA types in 2% (w/v) Poloxamer 188, corresponding PDI in hatched columns.

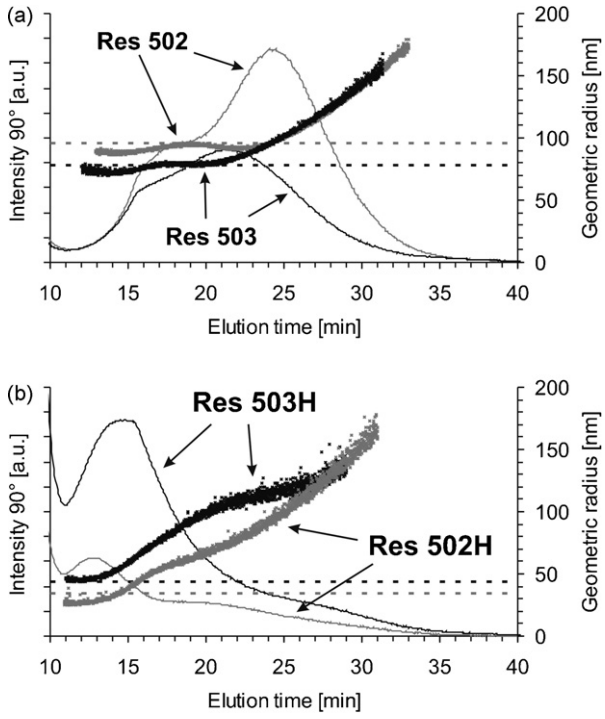

Fig. 6. FlFFF/MALS example fractograms of 0.25% (w/v) Resomer nanoparticles in 0.25% (w/v) Poloxamer 188: peaks represent scattering intensities at 90° and dots corresponding geometric radii, dotted horizontal lines display corresponding z-average radii from PCS.

SAXS to detect PLGA nanoparticle sizes. All the suspensions were produced under the same conditions. Consequently the resulting differences in particle size were caused by the respective polymer type. One varying parameter was the molecular weight. The corresponding values of all PLGA types are given in Table 1. Furthermore, the polymers differed in their end groups. The "H" at the end of the Resomer descriptions denoted the more hydrophilic substances with an unblocked –COOH end group.

The results for suspensions including 2% (w/v) Poloxamer 188 are shown in Fig. 5. A similar relationship in comparison to the hydrodynamic sizes received from SAXS was observed. Compared to SAXS, the PCS values had a slight tendency to higher values what can be explained by a water sorption layer influencing the particle diffusion but not influencing the radius of gyration. Comparing the values with those from nanosuspensions shown in Fig. 4, the particle sizes were slightly higher when Poloxamer was present. For the measured suspension of, e.g. Resomer RG 503, the diameter differences were calculated to be 7.5 nm for PCS and 8.0 nm for SAXS. Because only one suspension of each system was measured, these values were not sufficient to give statistically reliable information about a Poloxamer layer thickness.

3.4. FlFFF/MALS vs. PCS

Several PLGA nanosuspensions were characterized successfully and in a reproducible manner by FlFFF/MALS. Their fractograms are given in Fig. 6. Depending on the polymer type, peaks with different elution time and width were received. The

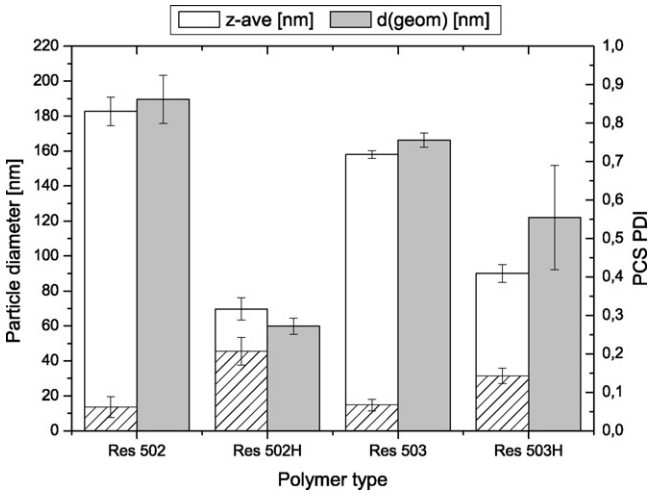

Fig. 7. Hydrodynamic (PCS) and geometric (FlFFF/MALS) diameters, corresponding PDI in hatched columns (suspensions from Fig. 6).

increasing size values with elution time indicated that smaller particles eluted first what is in accordance with the FlFFF theory [15]. Conspicuous were the differing elution profiles of Resomer 502/503 and 502H/503H. The latter had main peaks that reached their maxima already at elution times of approximately 13 or 15 min with a wide tail extending up to above 30 min. In contrast, Resomer 502/503 showed broad peaks with maxima at approximately 22 and 25 min with irregularly increasing sides, indicating a not completely monomodal distribution. Furthermore, a wide range of particle sizes up to a radius of almost 200 nm could be detected in all fractograms. Taking into account the detected maximum values, nanosuspensions had to be handled more carefully regarding a possible intravenous application. In contrast, the calculated average geometric diameters are displayed in comparison to the results from PCS in Fig. 7. The average values support the possibility of an intravenous injection of the nanoparticles. Furthermore, both methods detected sizes of the same order. The larger size differences of 502H and especially 503H could be attributed to their broader size distributions. This was indicated by their higher PDI values between 0.1 and 0.3 in contrast to values below 0.1 for the other suspensions. The width of the distributions resulted in different average values obtained by both methods due to the different measurement principles and the weighting

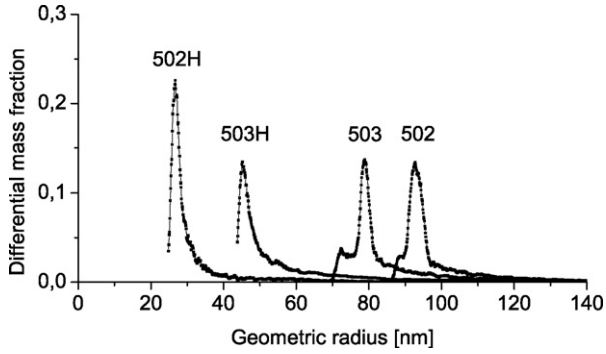

Fig. 9. Differential mass fraction vs. geometric radius derived from FlFFF/MALS (suspensions from Fig. 6).

on weight average (FFF/MALS) or scattering intensity (PCS), respectively.

The corresponding *z*-average radii are given as thin horizontal lines in Fig. 6. That allowed an evaluation of the FFF/MALS size region that was mainly detected by PCS. This was useful because light scattering batch methods as PCS are known to be limited to detect particles of different sizes in a mixture [23]. As it can be seen for the characterized suspensions, the *z*-averages were affected mainly by the FFF/MALS peak regions due to their high scattering intensity.

Particle size distributions could be derived from both techniques. A differential graph from PCS data is given in Fig. 8. Broad peaks appeared in the diameter range from approximately 20 nm up to above 400 nm. In contrast, in Fig. 9 the size distributions from FFF/MALS data are given. Compared to PCS, size distributions of higher quality were received. Most particles corresponded to a single size resulting in much sharper peaks. This can be explained by the FlFFF separation step prior to size detection. Furthermore, nanoparticles of 502 and 503 appeared to have slightly bimodal distributions indicated by small additional peaks at lower radii compared to those of the corresponding main peak.

To get comparable values of the above SAXS and PCS measurements, Resomer RG 503 nanoparticles were produced with 2% (w/v) and without Poloxamer 188. Sample fractograms from FlFFF measurements in respective background solvents are given in Fig. 10. In spite of the same used polymer type the same particle size fractions eluted much faster for nanosuspen-

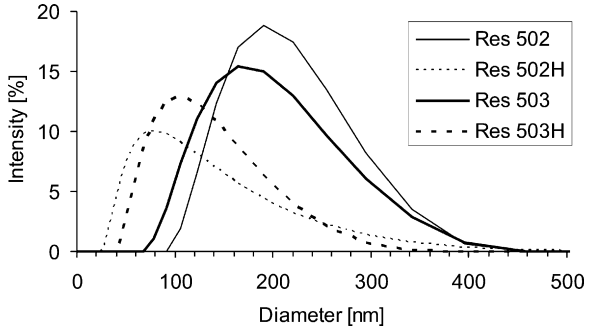

Fig. 8. Differential intensity distributions of *z*-average diameter from PCS (suspensions from Fig. 6).

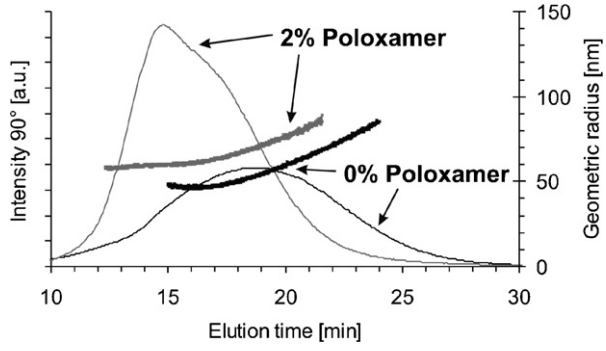

Fig. 10. FlFFF/MALS example fractograms of 0.5% (w/v) Res 503 nanosuspensions produced in 0% or 2% (w/v) Poloxamer 188 solution.

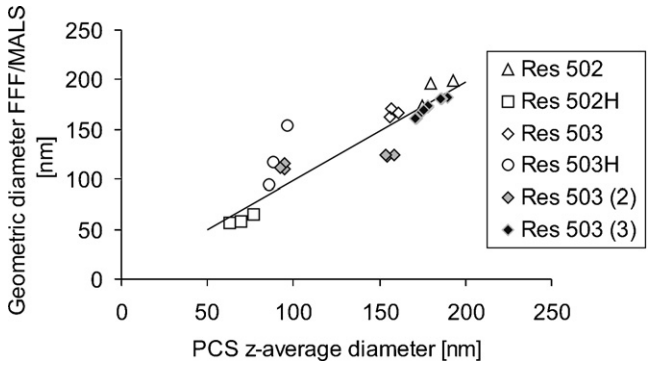

Fig. 11. Comparison of hydrodynamic (PCS) and geometric (FlFFF/MALS) PLGA nanoparticle sizes. The values were taken from nanosuspensions given in Fig. 10 (Res 503(2)) or 0.5% (w/v) Res 503 suspensions in 0.25% (w/v) Poloxamer 188 (Res 503(3)) or from Fig. 7 (all other PLGA suspensions). All values were basis for linear fitting.

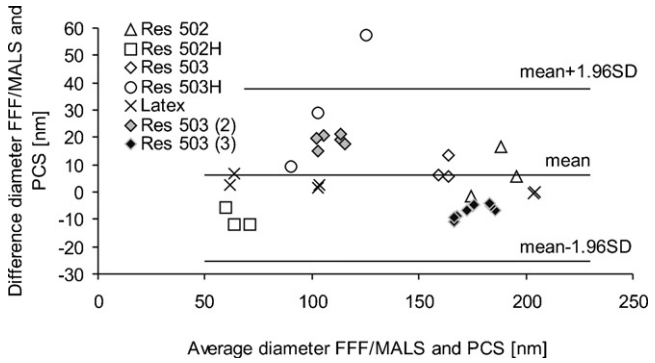

Fig. 12. Bland–Altman plot of same data and legends given in Fig. 11. PLGA values were basis for mean and standard deviation (S.D.) calculation, limits of agreement were 95%. Nanosphere latex data were taken from Ref. [12].

sions with Poloxamer. An explanation for this distance effect can be given either by a particle shell or a channel membrane covering of the Poloxamer. According to FlFFF theory of normal mode elution, due to the cross flow the particles were transported into the direction of the membrane during separation. The bigger the particles, the more they were influenced by the cross flow and the less they were able to diffuse back into the centre of the channel. As a result, smaller particles eluted faster during separation. However, Poloxamer might cover the channel or particle surface and prevent the particles to get closer to the membrane. Thus, the particles are pushed into a faster laminar flow, causing a faster elution through the channel. The average hydrodynamic diameters were found to be 94.5 ± 1.9 nm for the suspensions without and 104.2 ± 1.6 nm for the suspensions with poloxamer, resulting in a significant difference for a probability error $\alpha = 2.5\%$. The average geometric diameters from FFF/MALS were found to be 112.5 ± 2.7 nm for the suspensions without and 123.5 ± 0.9 nm for the suspensions with poloxamer, resulting in a significant difference ($\alpha = 2.5\%$). Thus, the differences in diameter caused by Poloxamer were 11.0 ± 2.9 nm for FFF/MALS and 9.8 ± 2.5 nm for PCS. These values were in a similar range as the one reported for SAXS compared to PCS (see Section 3.3). In addition the results of both techniques differed significantly ($\alpha = 2.5\%$), if poloxamer was used or not. Furthermore, the poloxamer containing nanosuspensions were separated in aqueous background without Poloxamer. A value of 120.2 ± 0.9 nm resulted what differed significantly ($\alpha = 2.5\%$) from the particles without Poloxamer in 7.7 ± 2.9 nm. Thus, at least a part of the Poloxamer layer was resistant to the intensive washing effect that appeared during the FlFFF focusing and separation steps. In comparison, for nanocapsule systems a radius difference of 17 ± 6 nm was reported for Poloxamer 188 [29]. This discrepancy can be explained by the different core materials, the different Poloxamer concentrations and different principles of detection methods.

In Fig. 11, all the PLGA nanosuspension size values are present to illustrate the agreement of size characterization in both methods. A linear fit of the geometric diameters from FlFFF/MALLS $d_{FFF/MALS}$ and z-average diameters from PCS d_{PCS} led to the following equation:

$$d_{FFF/MALS} = (1.03 \pm 0.02) \cdot d_{PCS} \quad \text{with} \quad R^2 = 0.835$$

The low R^2 can be explained by broader size distributions in several suspensions, leading to different values by both methods. For example, the points from Resomer RG 503H had corresponding PCS PDI values from 0.12 to 0.16 and do not seem to follow the linear relationship. In contrast, the PDI values of Resomer RG 502 ranged from 0.06 to 0.08, indicating a more narrow size distribution. Thus, their distance from a linear fitting curve was smaller. In comparison, values of monomodal sphere reference systems were given by us recently [12]. They displayed the excellent agreement of values from both methods for ideal monodisperse systems. As an alternative, in Fig. 12 the PLGA sphere values are displayed as a Bland–Altman plot. This plot is more advantageous to display values of different techniques for comparison and allows an easy investigation of relationship between discrepancies and the true value [30,31]. The ordinate mean value is 6.1 nm, what is slightly above the line of equality with an ordinate value of 0 nm. Thus, both measurements gave results of a similar magnitude but FFF/MALS apparently provided slightly higher values. A similar effect was already indicated for latex spheres in contrast to producer reference values [12]. The S.D. value was 16.1 nm, resulting in mean $\pm$ 1.96 S.D. lines of $\pm$31.6 nm in Fig. 12. When comparing the discrepancies at low and high average diameters, no difference shift could be recognized in the examined range.

Finally, it shall be mentioned that for all the light scattering techniques size values were calculated assuming homogeneous core systems. These findings cannot easily be extrapolated to non-ideal structures as, e.g. core shell systems. Then different sizes should be expected between average values from FlFFF/MALS, SAXS and PCS due to the small contrast difference from water but the high dimension of the outside layer.

4. Conclusion

In conclusion, PLGA nanosuspensions were produced using the solvent deposition method under selected conditions. Regularly shaped spherical particles were received what was proved

by TEM pictures and SAXS scattering curves. This information was necessary to calculate correct size values when using light scattering techniques. Dynamic viscosities were determined depending on the concentration of Poloxamer 188 that was used as a stabilizer. The received values enabled an exact calculation of hydrodynamic sizes received from PCS. Due to the moderate equipment demands and relatively short measuring time, PCS was chosen as a reference method for comparison with the other scattering techniques.

SAXS was performed at very low scattering angles using intensive synchrotron radiation. In spite of the high primary beam intensities, acquisition times exceeding 40 min had to be applied to the samples. On the other hand, due to short wavelength of the X-rays beam very small structures could be resolved. From small-angle data the particle sizes could be calculated. The results were in good agreement with z-average values obtained from PCS. Furthermore, the nanospheres were proven to be of spherical shape.

FlFFF/MALS separation was performed within more than 30 min using commercially available equipment. The received fractograms allowed an easy detection of maximum particle sizes what is the most important parameter for intravenous systems. Furthermore, this combination of apparatus provided size distributions of very high quality due to the separation step prior to size characterization. The calculated average size values exhibited a good correlation with z-averages determined by PCS. Only for suspensions of broader size distributions, higher deviations were observed with both techniques. The comparison of particle sizes with 2% (w/v) and without Poloxamer showed differences in diameters. The estimated discrepancies were 11.0 ± 2.9 nm for FFF/MALS and 9.8 ± 2.5 nm for PCS. These values were in a similar range as the ones obtained from SAXS. This corresponding additional shell could not be removed by intensive washing during FFF separation.

Thus, especially FlFFF/MALS has proved to be a valuable tool to characterize pharmaceutical nanosuspensions in detail what is of great importance especially for controlled drug delivery systems. Due to the pre-separation step it can be used as a good extension of PCS measurements. In spite of these advantages, up to now only a very limited number of literature resources are dealing with this combination of techniques within this field of research.

Acknowledgements

We want to thank Boehringer Ingelheim Pharma GmbH & Co. KG (Ingelheim, Germany) and PURAC biochem bv (Bingen, Germany) that kindly donated the different poly(D,L-lactide-co-glycolides) as BASF AG (Ludwigshafen, Germany) for the Poloxamer 188 and Microdyn Nadir (Wiesbaden, Germany) for the membranes. Furthermore, we are indebted to Mrs. Todte for the viscosity measurements. Additionally, we want to thank Dr. Metz (Institute of Pharmacy, Martin-Luther-University Halle-Wittenberg, Germany, Dr. Roessner (Wyatt Technology Europe) and Dr. Nietzsche (Malvern Instruments GmbH) for the helpful discussions.

References

[1] P. Markland, V.C. Yang, in: J. Swarbrick, J.C. Boylan (Eds.), Encyclopedia of Pharmaceutical Technology, Marcel Dekker, New York, 2002, pp. 136–155.
[2] H. Fessi, F. Puisieux, J.P. Devissaguet, N. Ammoury, S. Benita, Int. J. Pharm. 55 (1989) R1–R4.
[3] J. Molpeceres, M. Guzman, M.R. Aberturas, M. Chacon, L. Berges, J. Pharm. Sci. 85 (1996) 206–213.
[4] M. Chacon, L. Berges, J. Molpeceres, M.R. Aberturas, M. Guzman, Int. J. Pharm. 141 (1996) 81–91.
[5] H. Murakami, Y. Kawashima, N. Toshiyuki, H. Tomoaki, H. Takeuchi, M. Kobayashi, Int. J. Pharm. 149 (1997) 43–49.
[6] J. Vandervoort, A. Ludwig, Int. J. Pharm. 238 (2002) 77–92.
[7] S. Stolnik, L. Illum, S.S. Davis, Adv. Drug Deliv. Rev. 16 (1995) 195–214.
[8] S.E. Dunn, A.G.A. Coombes, M.C. Garnett, S.S. Davis, M.C. Davies, L. Illum, J. Control. Release 44 (1997) 65–76.
[9] S. Stolnik, S.E. Dunn, M.C. Garnett, M.C. Davies, A.G.A. Coombes, D.C. Taylor, M.P. Irving, S.C. Purkiss, T.F. Tadros, S.S. Davis, L. Illum, Pharm. Res. 11 (1994) 1800–1808.
[10] P. Couvreur, C. Dubernet, F. Puisieux, Eur. J. Pharm. Biopharm. 41 (1995) 2–13.
[11] J.C. Giddings, Science 260 (1993) 1456–1465.
[12] C. Augsten, K. Mäder, Pharm. Ind. 68 (2006) 1412–1419.
[13] W. Fraunhofer, G. Winter, Eur. J. Pharm. Biopharm. 58 (2004) 369–383.
[14] W. Fraunhofer, G. Winter, C. Coester, Anal. Chem. 76 (2004) 1909–1920.
[15] M.R. Schure, M.E. Schimpf, P.D. Schettler, in: M.E. Schimpf, K. Caldwell, J.C. Giddings (Eds.), Field-Flow Fractionation Handbook, Wiley Interscience, New York, 2000, pp. 31–48.
[16] H. Cölfen, M. Antonietti, Adv. Polym. Sci. 150 (2000) 67–187.
[17] P.J. Wyatt, J. Coll. Int. Sci. 197 (1998) 9–20.
[18] R.H. Müller, R. Schumann, Teilchengrößenmessung in der Laborpraxis, Wissenschaftliche Verlagsgesellschaft mbH, Stuttgart, 1996.
[19] O. Glatter, O. Kratky, Small Angle X-ray Scattering, Academic Press, London, 1982.
[20] B. Chu, T. Liu, J. Nanoparticle Res. 2 (2000) 29–41.
[21] Y. Nakata, Y. Takahashi, Drug Deliv. Syst. 15 (2000) 449–456.
[22] M.H.J. Koch, S.I. Svergun, A. Gabriel, B. Goderis, T. Unruh, Polym. Mater. Sci. Eng. 85 (2001) 173.
[23] O. Glatter, J. Sieberer, H. Schnablegger, Part. Part. Syst. Charact. 8 (1991) 274–281.
[24] O. Kratky, in: O. Glatter, O. Kratky (Eds.), Small Angle X-ray Scattering, Academic Press, London, 1982, pp. 3–13.
[25] G. Porod, in: O. Glatter, O. Kratky (Eds.), Small Angle X-ray Scattering, Academic Press, London, 1982, pp. 17–51.
[26] E. Cauchetier, M. Deniau, H. Fessi, A. Astier, M. Paul, Int. J. Pharm. 250 (2003) 273–281.
[27] D. Quintanar-Guerrero, E. Allemann, E. Doelker, H. Fessi, Colloid Polym. Sci. 275 (1997) 640–647.
[28] F. Ganachaud, J.L. Katz, Chem. Phys. Chem. 6 (2005) 209–216.
[29] A. Rübe, G. Hause, K. Mäder, J. Kohlbrecher, J. Control. Release 107 (2005) 244–252.
[30] J.M. Bland, D.G. Altman, Lancet 346 (1995) 1085–1087.
[31] J.M. Bland, D.G. Altman, Stat. Method Med. Res. 8 (1999) 135–160.
[32] C.G. Windsor, J. Appl. Cryst. 21 (1988) 582–588.